Aalborg Universitet

Field-Scale Monitoring of Urban Green Area Rainfall-Runoff Processes

Nielsen, Kristoffer; Møldrup, Per; Thorndahl, Søren Liedtke; Nielsen, Jesper Ellerbæk; Uggerby, Mads; Rasmussen, Michael R.

Field-Scale Monitoring of Urban Green Area Rainfall-Runoff Processes

Kristoffer T. Nielsen[1]; Per Moldrup, Ph.D.[2]; Søren Thorndahl, Ph.D.[3]; Jesper E. Nielsen, Ph.D.[4]; Mads Uggerby[5]; and Michael R. Rasmussen, Ph.D.[6]

Abstract: Rainfall-runoff-generating mechanisms in urban green areas are scarcely understood, and limited knowledge and data on rainfall-runoff processes are available. Therefore, a large-scale experimental field station was established to investigate the inherent hydrological processes of a grass-covered 4,300 m² urban catchment consisting of sandy loam soil. A facility to collect surface runoff from the area was designed. Runoff, soil moisture properties, and rainfall were measured simultaneously by a flow meter, in-ground soil sensors, and rain gauges, respectively. Measured soil volumetric water content was above 0.34 m³ H_2O m^{-3} soil during fall and winter and ranging between 0.13 and 0.34 m³ H_2O m^{-3} soil during late spring and summer. Measured runoff recorded from September 2016 until July 2018 strongly indicates that subsurface throughflow was the dominant runoff type. There was good correlation between the dynamics of soil water content and runoff. Accumulated rainfall and runoff was linearly correlated for soil volumetric water contents above 0.34 m³ H_2O m^{-3} soil. The relationship between runoff and rainfall shows a runoff coefficient of 0.18 for the 4,300 m² area. **DOI: 10.1061/(ASCE)HE.1943-5584.0001795.** *This work is made available under the terms of the Creative Commons Attribution 4.0 International license, http://creativecommons.org/licenses/by/4.0/.*

Author keywords: Urban drainage; Rainfall-runoff from green areas; Pervious surface; Permeable; Infiltration; Subsurface throughflow.

Introduction

Rainfall-runoff from urban green areas can potentially contribute with significant runoff loads to urban drainage networks. Nevertheless, Redfern et al. ([2016](2016)) acknowledge that studies and research on this topic are limited; hence, accurately assessing the hydrological impact from urban green areas is a difficult task. Boyd et al. ([2009](2009), [1994](1994)) studied rainfall-runoff from urban green areas on urban catchment scales. However, more research is needed for deeper understanding as urban green surface runoff could increase uncertainty in urban drainage modeling (Thorndahl et al. 2006, [2008](2008)). Generally, runoff from urban green areas is dependent on a variety of parameters, and without empirical knowledge, it is difficult to qualitatively estimate the runoff load from these areas. In the design of urban drainage systems, this can result in wrong assumptions, leading to either under- or overestimation of the runoff load from urban green areas. The consequence of this is either too high construction costs in the case of overestimation or too high flood damage costs in the case of underestimation. Therefore, empirical knowledge is crucial to improve future assumptions regarding infiltration and runoff models for urban green areas.

Infiltration excess models such as Horton's infiltration equation (Horton 1939) and the Green–Ampt model (Green and Ampt 1911) are widely used to estimate rainfall-runoff from permeable surfaces. These models assume that if the rainfall intensity exceeds the infiltration capacity, the excess will cause surface runoff. This runoff is known as infiltration excess overland flow and has always been considered the primary hydrological process for generating rainfall-runoff from permeable surfaces. However, studies have shown that permeable runoff is more diverse (Dunne and Black 1970a, [b](b); Kirkby and Chorley 1967). Generally, permeable runoff can be grouped into three processes: (1) infiltration excess runoff, (2) saturation excess runoff, and (3) subsurface throughflow. All three types are observed in a field study by Pilgrim et al. ([1978](1978)). However, other field studies have not been able to detect infiltration excess overland flow as a contributor of rainfall-runoff from permeable surfaces (Dunne and Black 1970a, [b](b); Kirkby and Chorley 1967). More empirical knowledge about these hydrological processes will improve both the design and modeling of urban drainage networks. Such observations can be implemented in both model calibration and in data-driven models such as in data assimilation (Brocca et al. 2009) and artificial neural networks for hydrological applications (ASCE Task Committee on Application of Artificial Neural Networks in Hydrology 2000; Govindaraju 2000).

In empirical case studies from forest, agricultural areas, and laboratory studies, rainfall simulators are a widely used method to estimate runoff, erosion, nutrient transport, and other runoff-related mechanisms (Benavides Solorio and MacDonald 2001; Cerdà et al. 1997; Clarke and Walsh 2007; Humphry 2002; Ribolzi et al. 2011; Sharpley 2003; Shuster et al. 2008). However, with artificially generated rainfall, rain and soil interactions may not always be realistic. Therefore, large-scale studies are important to understand how small-scale rainfall simulator studies can be interpreted and scaled in relation to urban catchments.

[1]Industrial Ph.D. Student, Dept. of Civil Engineering, Aalborg Univ., Thomas Manns Vej 23, Aalborg 9220, Denmark; Industrial Ph.D. Student, EnviDan A/S, Vejlsøvej 23, Silkeborg 8600, Denmark (corresponding author). Email: kni@civil.aau.dk

[2]Professor, Dept. of Civil Engineering, Aalborg Univ., Thomas Manns Vej 23, Aalborg 9220, Denmark.

[3]Associate Professor, Dept. of Civil Engineering, Aalborg Univ., Thomas Manns Vej 23, Aalborg 9220, Denmark.

[4]Associate Professor, Dept. of Civil Engineering, Aalborg Univ., Thomas Manns Vej 23, Aalborg 9220, Denmark.

[5]Head of Research and Development, EnviDan A/S, Vejlsłvej 23, Silkeborg 8600, Denmark.

[6]Professor with Specific Responsibilities, Dept. of Civil Engineering, Aalborg Univ., Thomas Manns Vej 23, Aalborg 9220, Denmark.

Various factors have the potential to affect rainfall-runoff in urban environments. Pan and Shangguan (2006) found that grass cover reduces surface-runoff generation compared to bare soils. However, Quinton et al. (1997) found no significant relationship between the type of plant cover and runoff generation, except that plant cover generally reduces runoff. Quinton et al. (1997) further found that generated runoff decreases by increased canopy cover. Soil water content also affects permeable runoff and has been used to improve runoff prediction models (Jacobs et al. 2003). Grayson (1997) indicated that horizontal or vertical water transport processes in the soil could be detected depending on the spatial uniformity of soil water content. Furthermore, properties of soil types can significantly affect the infiltration capacity (Groenendyk et al. 2015). Some areas in urban environments suffer from degraded infiltration capacity due to heavy soil compaction caused by urban activity, for example, road and building constructions (Gregory 2006). Finally, morphological properties such as the slope and length of a catchment also affect the amount of runoff from permeable surfaces (Sharma 1986).

In the present study, a large-scale experimental field station is designed to measure rainfall-runoff from an urban green catchment. Simultaneously, soil water properties and rainfall are measured on site. Furthermore, a comprehensive study of the basic soil water properties and soil characteristics are investigated. The scope is to evaluate whether rainfall-runoff is present from a relatively common type of urban surface (grass covered park in a residential area). Studying the runoff processes on a large scale makes it possible to evaluate how urban green area rainfall-runoff responds as a result of hydrological mobilization of an entire catchment. This is contrary, for example, to rainfall simulation studies that only study runoff processes in areas of approximately 1 m^2, which could lead to boundary effects affecting measured runoff. Furthermore, this study will be a reference study to urban green surface runoff studies because similar such experiments in urban environments are scarce, whereas only a few such experiments have been carried out in rural areas. Finally, it is the goal of this study to obtain qualitative hydrographs to examine the relationship between rainfall and permeable runoff. Thus, the correlation between soil water properties and rainfall-runoff is studied to assess whether such measurements have a potential use in urban drainage design.

Materials and Methods

The field station is established in the city of Lystrup, Denmark, to collect rainfall-runoff from a 4,300 m^2 permeable catchment (Fig. 1) with an average slope of 8.8%. Before urban development, the land was used as agricultural farmland until the 1960s. The monitored area in Lystrup is a recreational park surrounded by residential houses. The field station is equipped with a slope-intercept line drain (Fig. 1) that collects surface runoff and measures the discharge from the catchment with a flow meter. Furthermore, three clusters of soil sensors are established for measuring soil volumetric water content (VWC) and matric potential (MP). The soil sensor clusters will be further denoted as the bottom, middle, and top sensor clusters. Finally, a tipping bucket rain gauge monitors the rainfall. All sensors are connected to battery-driven YDOC ML-315ADS-Li data loggers (YDOC 2016, Bennekom, The Netherlands), and data are transferred through a mobile broadband connection to a file transfer protocol (FTP) server in real time. The field station has been collecting data since September 2016 and is still active. Data included in this study extend from September 2016 to July 2018.

The field station measures some of the central parameters used in traditional surface runoff modeling. Eq. (1) presents a simple continuity equation that shows the primary processes that affects the accumulation of water on a permeable surface:

$$A\frac{dy}{dt} = PA - Q(y) - fA \qquad (1)$$

where A (m^2) = catchment surface area; y (m) = ponding water level on soil surface; t (s) = time; P (ms^{-1}) = precipitation; Q (m^{3}s^{-1}) = surface runoff rate; and f (ms^{-1}) = infiltration rate. Precipitation is the input source of water to the runoff model, while the surface runoff rate and infiltration rate discharges water from the model. Precipitation and the runoff rate can be measured directly, while the infiltration rate is more difficult to measure. However, infiltration depends on the soil water content and matric potential. Therefore, these parameters can be used as indirect indicators of infiltration. In urban drainage modeling, various simplified approaches are typically used to model the vertical infiltration capacity of a permeable surface. The Green–Ampt model is one of the most commonly used models and describes the infiltration rate as a function of time (Green and Ampt 1911; Kale and Sahoo 2011):

$$f(t) = K\left(1 + \frac{h_0 + h_s}{L}\right) \qquad (2)$$

where K (ms^{-1}) = saturated hydraulic conductivity; h_0 (m) = depth of ponding water level on soil surface; h_s (m) = capillary suction head or matric potential at wetting front; and L (m) = distance to wetting front. The matric potential depends on the soil water content. As seen, runoff, precipitation, soil water content, and soil matric potential can therefore be used to describe the primary processes that could affect rainfall-runoff from the 4,300 m^2 permeable catchment in Lystrup.

Surface Runoff Collection and Flow Meter

A cross-sectional view of the surface runoff collection facility is presented in Fig. 2. First, surface runoff is collected in a 51 m long, concrete-reinforced, ACO HexaLine line drain (ACO Nordic 2014, Ringsted, Denmark). The collected water is transported through a grit chamber to remove dirt and particles before reaching a V-notch weir that measures the discharge. The current water level in the V-notch weir is logged every 5 min and converted into flow estimates with a calibrated Q–h relation. The water level is measured with two Campbell Scientific CS451 pressure transducers (Campbell Scientific 2014, Logan, UT).

Soil Sensors

Three soil sensor clusters equipped with four sensors each measure different soil water properties every 15 min. The sensors in each cluster are located within a few meters from each other. The following sensor types are installed to monitor soil water content and soil matric potential:
- Five Decagon 5TE sensors (Decagon Devices 2016, Pullman, WA) measuring soil volumetric water content; two are located at the top sensor cluster, two at the middle sensor cluster, and one at the bottom sensor cluster.
- Four Decagon MPS6 sensors (Decagon Devices 2015, Pullman, WA) measuring soil matric potential (range 1.96–6.01 pF); one is located at the top soil sensor cluster, two at the middle soil sensor cluster, and one at the bottom soil sensor cluster.
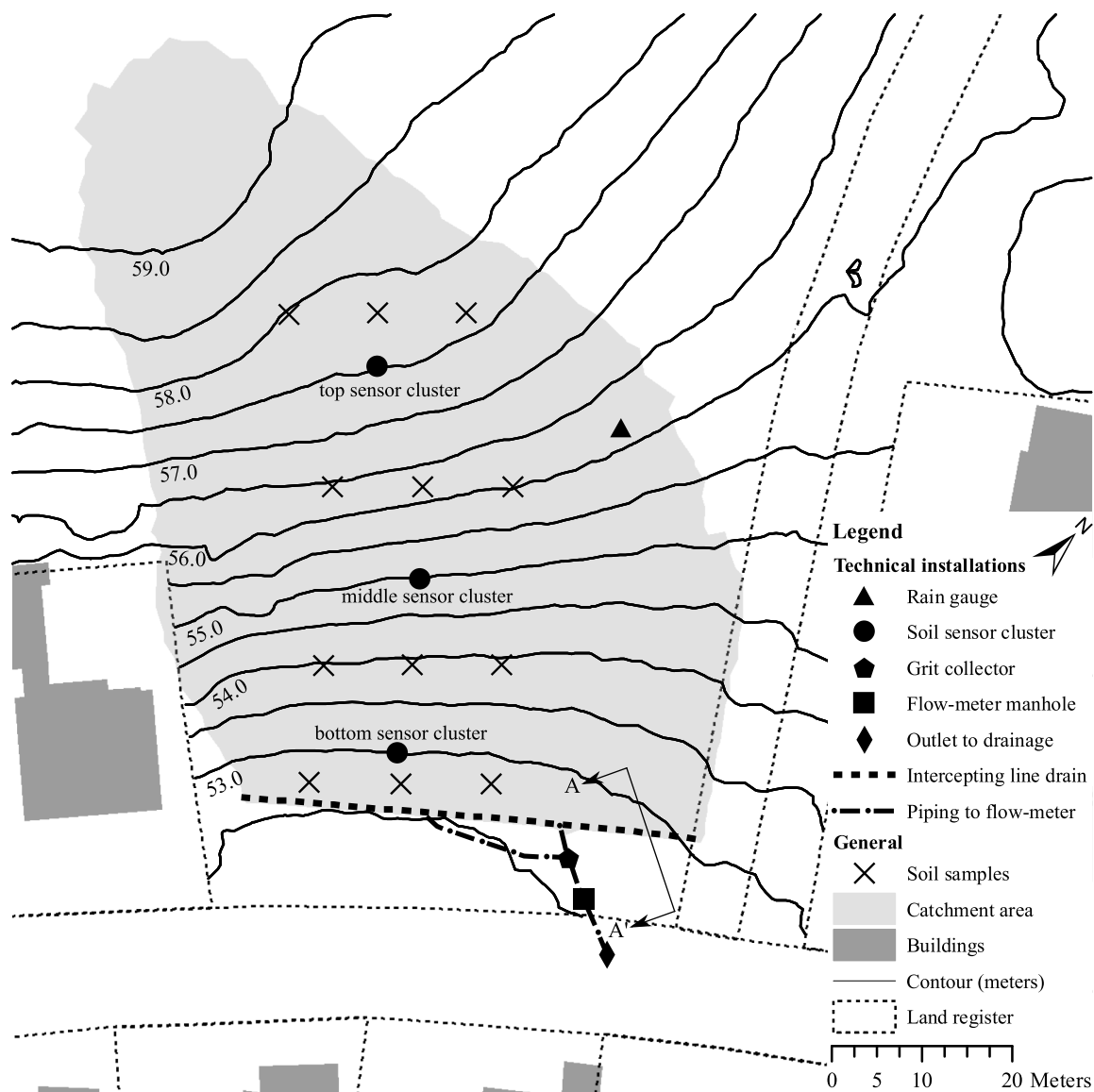
Fig. 1. Study area in Lystrup, Denmark. Location at 56.23, 10.22 (latitude, longitude). The catchment covers an area of 4,300 m². Cross Section A–A′ of water collection system is seen in Fig. 2.

- Two Stevens TensioMark (Portland, OR) sensor (ecoTech Umwelt-Meßsysteme 2014) measuring soil matric potential (range 0–2.85 pF); each of the top and bottom soil sensor clusters have one of these installed.
- One Sentek SDI-12 Drill & Drop Probe (Stepney, South Australia) (Sentek 2015) measuring soil volumetric water content at nine different depths from −5 to −85 cm. This sensor is located at the bottom sensor cluster.

Rain Measurement

Rainfall is measured with a triple rain gauge setup with three colocated tipping bucket rain gauges mounted on one stand. In this way, the measurement uncertainty is reduced, and it gives the opportunity to compare the performance of each rain gauge constantly. The tipping bucket rain gauges are of the ARG100 type (Campbell Scientific 2010, Logan, UT) and measure 0.2 mm tip⁻¹ in time increments of 1 min. In general, the rain gauges show little intervariation in measured rainfall. The setup had to be moved from its original location (Fig. 1) to a new location in the period July 2–12, 2017,

to avoid vandalism. After the July 12, 2017, the rain gauges were set up on a private estate 400 m northwest of the original location.

Soil Characterization

A total of 23 intact samples from a depth of 10 cm were used for soil characterization. Dry bulk density and total porosity of soil samples are determined by drying at 105℃. Effective porosity is measured using a pressure plate apparatus (Dane and Topp 2002). Average organic matter content is estimated by ignition loss on six samples at 550℃ in a muffle oven.

Soil layering near the surface is investigated with a soil profiler to 100 cm depth at 12 points. Soil texture is classified at 10 cm depth by wet sieving analysis of six samples, which separates sand particles from silty and clayey particle fractions. Another three wet sieving analyses are carried out on soil samples sampled in deeper soil layers. Two hydrometer tests are performed in both the top layer and deeper soil layers to estimate the clay content. The soil texture is finally classified according to the USDA soil classification system (Ashman and Puri 2013).
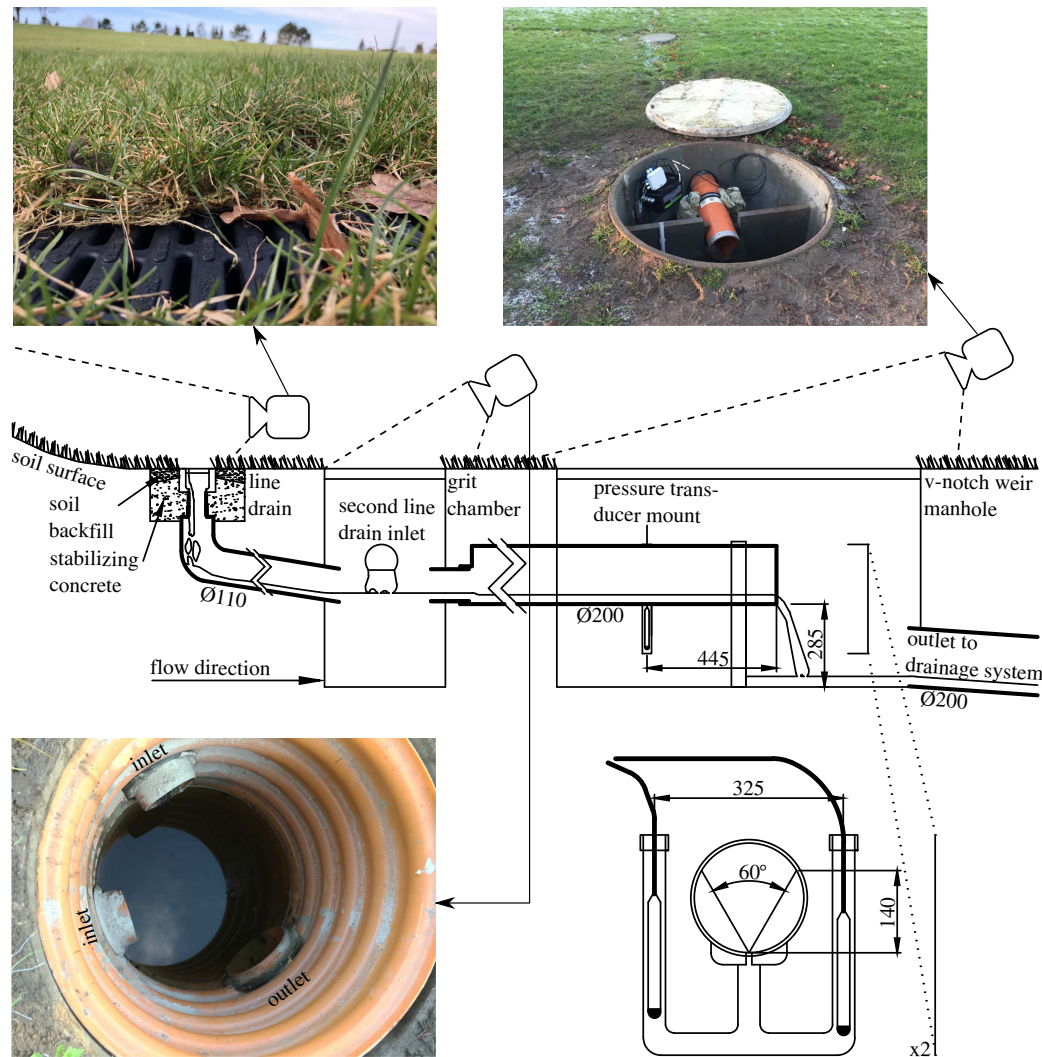
Fig. 2. Cross-sectional view of Section A–A′ in Fig. 1 of water collection system (dimensions in millimeters).

Infiltrometer tests are carried out on 12 locations with a double-ring infiltrometer designed according to the criteria given by Arriaga et al. (2010). Consequently, the saturated hydraulic conductivity, K_{fs} (cm min^{-1}), can be derived according to (Dane and Topp 2002)

$$K_{fs} = \frac{q_s}{\frac{H}{C_1 d + C_2 a} + \frac{1}{\alpha^*(C_1 d + C_2 a)}} + 1 \qquad (3)$$

where q_s (cm min^{-1}) = quasi-steady infiltration rate; H (cm) = water ponding depth; d (cm) = insertion depth of infiltrometer; a (cm) = inner-ring radius of double-ring infiltrometer; α^* (cm^{-1}) = macroscopic capillary length of soil; and C_1 and C_2 are quasi-empirical constants. For calculations of the saturated hydraulic conductivity in this study $d = 10$ cm, a $= 15$ cm, $\alpha^* = 0.12$ cm^{-1}, $C_1 = 0.316\pi$, and $C_2 = 0.184\pi$. H and q_s vary within each infiltrometer test.

Obtained values of average effective porosity and saturated hydraulic conductivity are subsequently validated by the empirical relationship of common soil types between effective porosity, ε_{100}, and saturated hydraulic conductivity, K_s (cm day^{-1}), derived by Poulsen et al. (1999):

$$\log(K_s) = 2.8 \log(\varepsilon_{100}) + 4.3 \qquad (4)$$

Results

Soil Characteristics

Fig. 3 shows the distribution of dry bulk density, total porosity, and effective porosity at a depth of 10 cm, and the saturated hydraulic conductivity of the topsoil. It is evident that there is a significant spatial variation in the soil parameters at the site. However, the saturated hydraulic conductivity is more homogeneously distributed. In general, the topsoil layer yields an average dry bulk density of 1.52 g cm^{-3}, total porosity of 0.43, effective porosity of 0.18, saturated hydraulic conductivity of 1.10 mm min^{-1}, and average organic matter content of 5.06%. This composes a topsoil with a relatively high infiltration capacity and high organic matter content.

According to Eq. (4), the calculated saturated hydraulic conductivity is 1.14 mm min^{-1} using a measured average effective porosity of 0.18. Compared to the average of the measured conductivity, it is a deviation of 3.8%, indicating that the quality of the sampling is high.

A layer transition is found at an average depth of 46 cm. The organic matter content in the lower layer is significantly lower at 1.34%. However, the soil texture in both layers is relatively similar (Fig. 4), and both layers are sandy loams according to the USDA soil classification system. However, the lower soil layer does seem
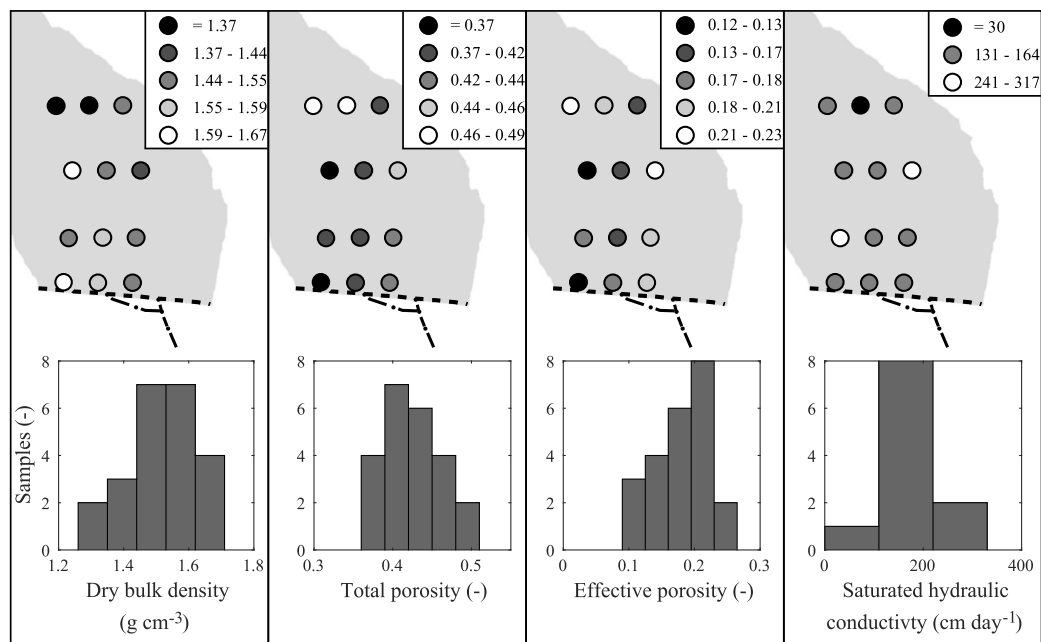
Fig. 3. Spatial distribution of dry bulk density, total porosity, effective porosity, and saturated hydraulic conductivity at 12 sampling points. Below each spatial distribution map a histogram shows the sampling distribution of 23 intact samples (saturated hydraulic conductivity is based on 12 infiltrometer tests).

to contain slightly more silt. Combined with a higher soil compaction at this depth, this could result in a lower effective porosity and thereby lower the infiltration capacity compared to the topsoil.

Variation of Soil Volumetric Water Content and Distribution of Accumulated Rainfall

According to Fig. 5, soil volumetric water content is high from September until May. In the period from April until August, greater variation in soil water content is observed at lower values.

Observed Rainfall-Runoff and Soil Water Content Dynamics

From September 2016 to July 2018, 14 significant rainfall events (Table 1) were recorded. Six events contributed significantly to
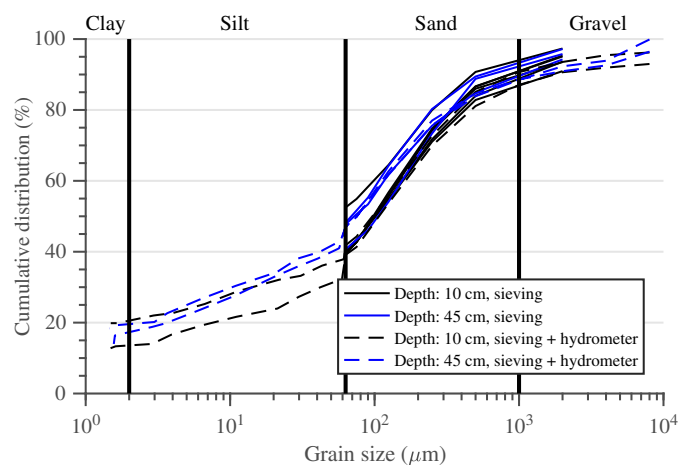

Fig. 4. Grain size distribution of soil samples from 10 and 45 to 50 cm depth derived on both wet sieving analysis and hydrometer tests.

surface runoff from the green area, while some events produced limited or close to no runoff. Runoff events occur during fall and winter caused by long-lasting precipitation with relatively low rainfall intensity. The runoff period is significantly longer than the rainfall duration. The runoff duration is observed to be between 2 and 16 days. The severity of the rainfall is expressed by the largest return period of rainfall events precipitating within the runoff in terms of intensity-duration-frequency according to Danish rainfall statistics (Madsen et al. 2017).

Rainfall Events c and d (Table 1) reach return periods of 10 and 7 years for rainfall durations of 0.5 and 12 h, respectively. Event c is a short-term convective cloudburst (above 15 mm rainfall within 30 min), and Event d is a long-term frontal passage with stratiform rainfall. Measurements showed that the cloudburst (Event c) did not produce significant contributions to runoff. In contrast, the frontal rainfall produced significant runoff.

The dynamics of some selected significant rainfall-runoff events are presented in Fig. 6. These events are primarily the result of periods with combined rainfall events where rainfall prior to the event has not completely infiltrated. Instead, rainfall events occurring within short intervals maintain a high soil water content and thereby increases the probability of further rainfall to produce surface runoff.

Runoff Events a, d, and g (Fig. 6) demonstrate similar patterns where an initial relatively large rainfall event triggers the runoff. Event i in Fig. 6 differs from other events as runoff increases during consecutive rainfall events causing the runoff to reach higher rates for each rainfall event. Runoff starts to decrease as soon as rainfall occurs with larger intervals.

Generally, all significant rainfall-runoff events start when the soil water content is high. Events c, d, and n (Table 1) start at lower soil water contents than the other events. Event n is unique as snowmelt causes runoff. Therefore, Event n is not considered further in the study of rainfall-runoff relationships.

Soil volumetric water content measured in the soil sensor clusters (VWC bottom, middle, and top in Fig. 6) shows good correlation with observed rainfall-runoff. When soil water content
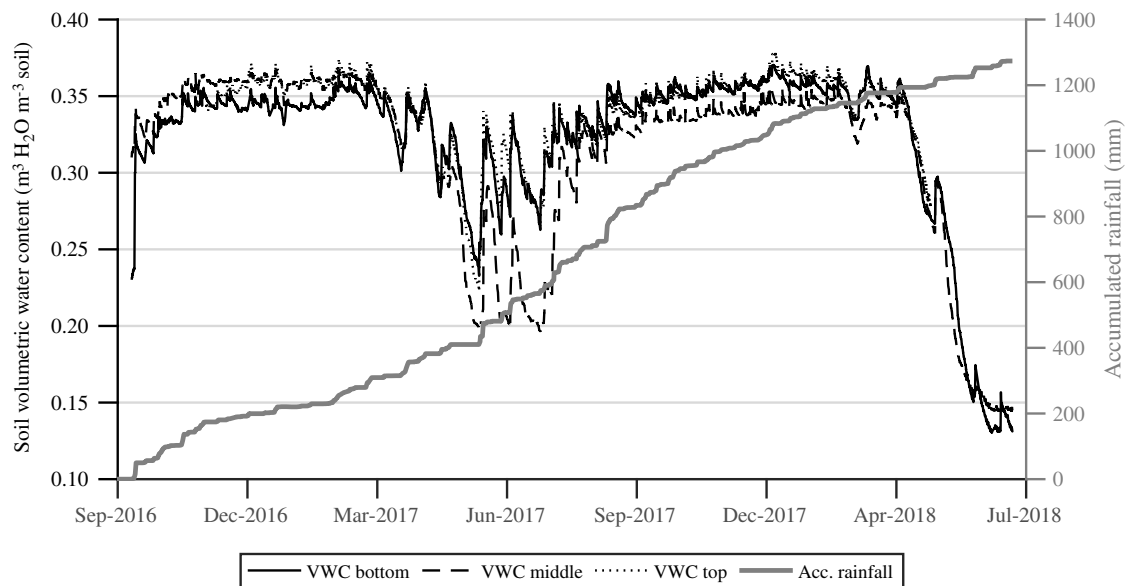
Fig. 5. Variation of measured soil volumetric water content in bottom, middle, and top sensor clusters presented in Fig. 1 and accumulated rainfall in Lystrup recorded in period September 2016–July 2018. Due to a malfunctioning data logger, no data for VWC top were recorded in period April 2018–July 2018.

Table 1. Summary data of measured significant rainfall and runoff events, September 2016–July 2018

				Recorded rainfall-runoff events				
Event	Event start	Runoff duration (days)	Total precipitation (mm)	Precipitation type	Return period (year)	Total runoff (mm)	Runoff percentage	Initial volumetric water content ($m^3 H_2O\,m^{-3}$ soil)
a	November 4, 2016	10.5	40.3 ± 1.0	Rain	<1	7.4	18.4	0.34
b	November 14, 2016	9.5	30.8 ± 0.7	Rain	<1	4.9	15.9	0.35
c	July 30, 2017	<0.1	22.4 ± 0.2	Cloudburst	10 (t_{dur} = 0.5 h)	~0	~0	0.30
d	September 5, 2017	16.2	102.9 ± 0.3	Rain	7 (t_{dur} = 12 h)	12.7	12.3	0.32
e	October 4, 2017	2.9	10.0 ± 0.0	Rain	<1	0.1	1.0	0.34
f	October 7, 2017	2.2	5.8 ± 0.0	Rain	<1	~0	0.6	0.34
g	October 11, 2017	2.0	15.9 ± 0.1	Rain	<1	0.4	2.3	0.34
h	October 21, 2017	2.2	9.5 ± 0.2	Rain	<1	0.1	1.4	0.34
i	October 24, 2017	5.6	24.6 ± 0.5	Rain	<1	1.7	6.8	0.35
j	November 1, 2017	1.7	7.5 ± 0.1	Rain	<1	0.1	0.7	0.34
k	November 21, 2017	9.3	23.5 ± 0.2	Rain	<1	3.8	16.1	0.35
l	January 15, 2018	4.9	12.0 ± 0.0	Rain	<1	~0	0.1	0.35
m	January 23, 2018	3.8	8.6 ± 0.2	Rain	<1	~0	0.2	0.35
n	March 5, 2018	9.8	—	Snowmelt	—	5.9	—	0.33

Note: Event duration is based on approximate trigger of runoff and the end at which the runoff rate reaches approximately zero flow; total runoff (mm) is calculated using a catchment area of 4,300 m^2; t_{dur} = rainfall duration of return period.

increases, the runoff rate does, too. Furthermore, slowly declining runoff is comparable to slowly declining soil water content. During strong runoff peaks, the bottom sensor cluster (VWC bottom in Fig. 6) shows a different relationship between soil water content and runoff than the other soil sensor cluster. During peak runoff rates, the water content in the bottom sensor cluster stagnates briefly. This is an indication of near saturated conditions in the soil at the bottom of the hill, which further indicates that subsurface throughflow is discharging water to the surface. Furthermore, near saturated conditions at the bottom of the hill could also be an indicator of wet spots causing direct runoff known as saturation excess runoff. Therefore, the bottom hill soil sensor cluster shows the best correlation to strong runoff peaks.

It seems that matric potential (MP in Fig. 6) is more dynamic compared to soil volumetric water content and reaches zero in some

periods. This indicates that the soil is fully saturated. The soil matric potential does not increase or decrease in the same way as the soil water content does compared to runoff. Instead, it is observed that during periods of high runoff rate, the matric potential tends to rapidly reach zero and stay there until the runoff rate decreases. This is because near saturated soil conditions increase subsurface throughflow as flow in the soil pores is activated due to a water storage deficit in the soil.

The rainfall-runoff events possess similar characteristics regarding which criteria need to be fulfilled before surface runoff starts. Considering the initial phase of Event d (Fig. 7), it is seen that the soil must reach a certain soil water content before runoff starts. This happens between Points P1 and P2, which are marked as focus points in Fig. 7, where the average soil volumetric water content rises to approximately 0.34 $m^3 H_2O\,m^{-3}$ soil. At P2 to P3 (Fig. 7),
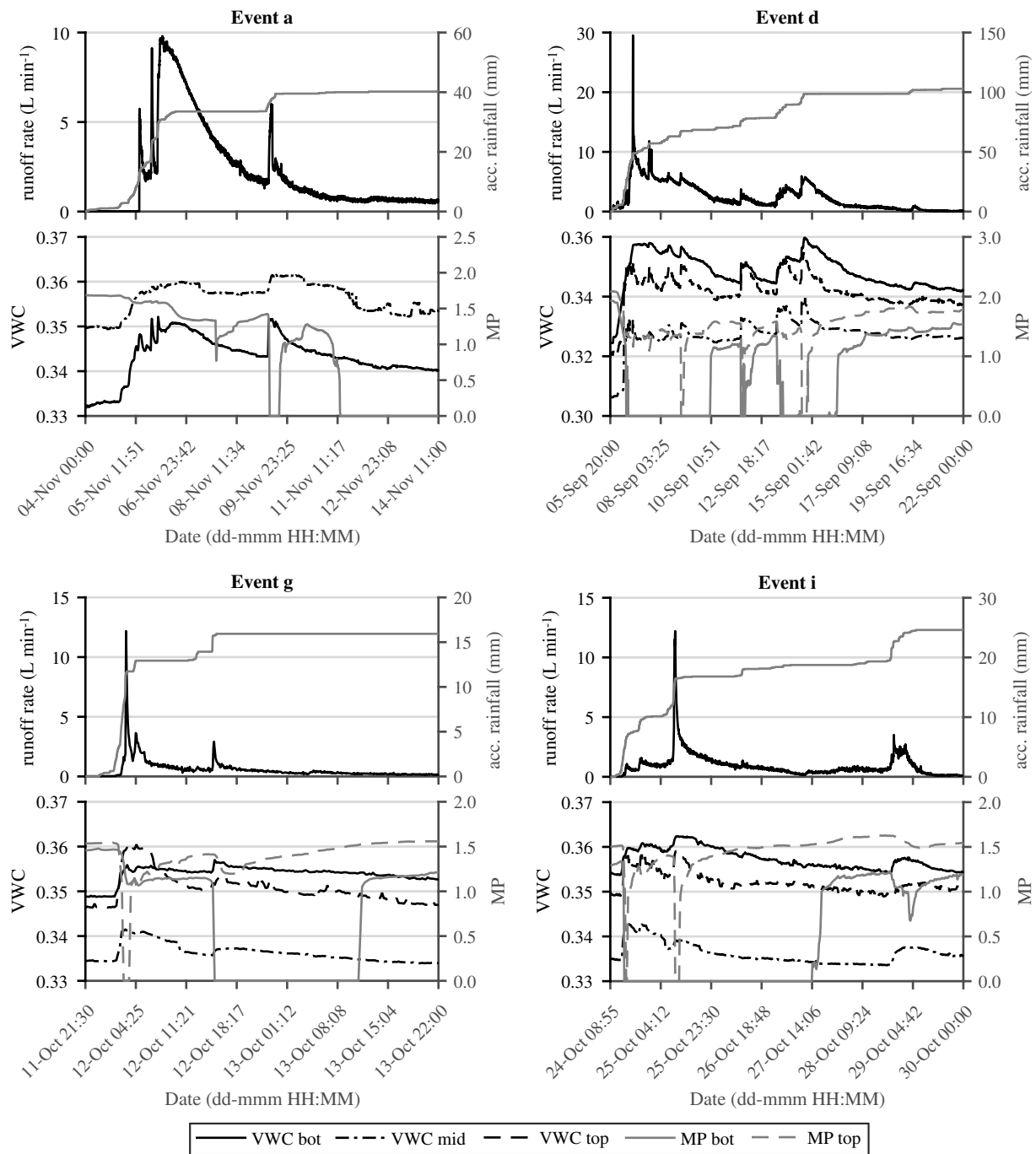
Fig. 6. Events A, D, I, and G presented in Table 1. Measured rainfall, runoff, soil volumetric water content [VWC ($m^3\,H_2O\,m^{-3}$ soil)], and matric potential {MP [Log(-soil-water matric potential in centimeters of water head)]}. Volumetric water content bottom, middle, and top represent measured soil volumetric water contents at bottom, middle, and top soil sensor clusters, respectively. Matric potential bottom and top represent MP measured in bottom and top soil sensor clusters. No sensors were installed in the top sensor cluster during Event A.

runoff seems to be triggered and starts to produce significant runoff. After P3, the runoff response to precipitation seems to become increasingly sensitive as relatively small amounts of rainfall cause a relatively high spike in the runoff rate. At the time of the runoff spike, the soil water content in VWC bottom (Fig. 7) stagnates. This indicates that the soil could be at or near a fully saturated state in the bottom sensor cluster. Between P3 and P4, the runoff rate decreases due to less rainfall with only small runoff increases due to rainfall. Generally, the same patterns seem to be present for all rainfall-runoff events. The average soil volumetric water content

of all soil sensor clusters needs to be above 0.34 $m^3\,H_2O\,m^{-3}$ soil before runoff starts, and during high runoff spikes, the soil water content at the bottom hill sensor cluster stagnates.

Runoff Coefficient for Surface Runoff from Green Areas

Significant runoff does not start unless the soil volumetric water content exceeds 0.34 $m^3\,H_2O\,m^{-3}$ soil. Compared to the average total porosity of 0.43, and locally as low as 0.37, this is a relatively wet
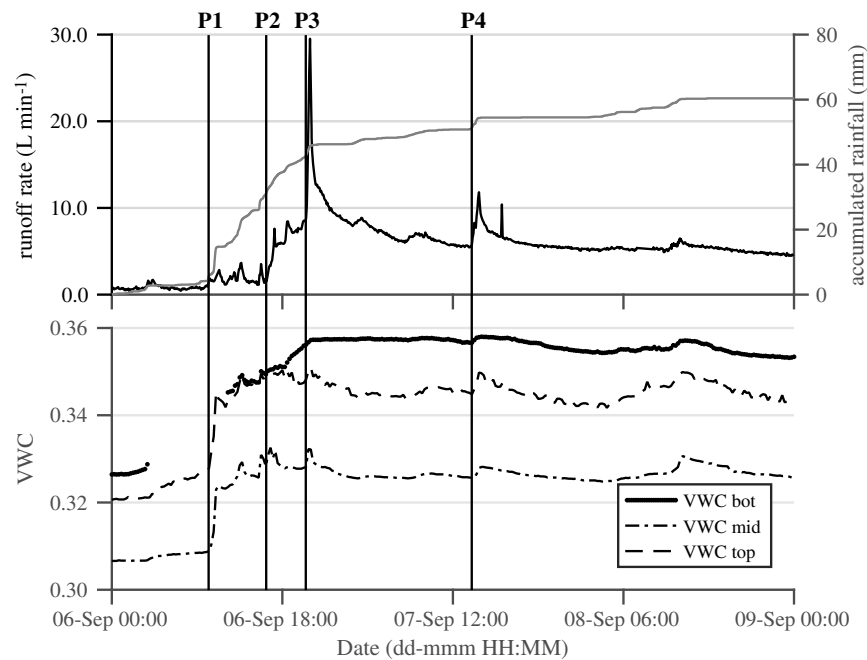
Fig. 7. Detailed illustration of initial phase of rainfall-runoff Event D (Table 1). Numbered vertical lines indicate special focus points (P1–P4) in terms of rainfall-runoff-generating mechanisms.
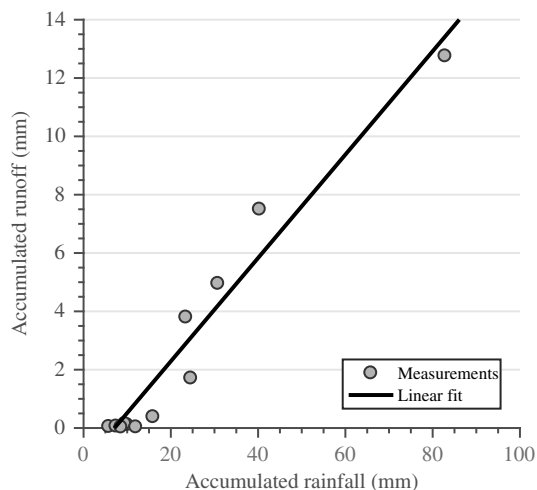

Fig. 8. Accumulated runoff model for soil water contents above $0.34 \text{ m}^3 \text{ H}_2\text{O m}^{-3}$ soil. The regression has a correlation coefficient of $R^2 = 0.92$.

state in the soil. Therefore, the relationship between accumulated runoff and rainfall is investigated only for rainfall and runoff occurring above soil volumetric water contents of $0.34 \text{ m}^3 \text{ H}_2\text{O m}^{-3}$ soil. This is illustrated in Fig. 8, where measured rainfall with accumulated rainfall volumes smaller than 15 mm occurring at soil volumetric water contents above $0.34 \text{ m}^3 \text{ H}_2\text{O m}^{-3}$ soil produces no runoff. The remaining measurements with accumulated rainfall volumes higher than 15 mm produce significant runoff and show a linear relationship between accumulated rainfall and runoff. Therefore, runoff events with accumulated rainfall depths below 15 mm are not included to form the linear regression between accumulated rainfall, P_{tot} (mm), and runoff, V_{tot} (mm), presented in Fig. 8 and Eq. (5):

$$V_{tot}(P_{tot}) = 0.18 P_{tot} - 1.26 \qquad (5)$$

The linear regression expresses the amount of runoff that can be expected as a function of the accumulated rainfall if the soil volumetric water content is above $0.34 \text{ m}^3 \text{ H}_2\text{O m}^{-3}$ soil. The regression can be further used to explain some of the basic hydrological processes occurring from the hill in Lystrup. The intercept of the x-axis shows that an initial loss of 7.1 mm is present according to the linear theory between rainfall and runoff. This differs from the initial loss of 15 mm based only on measurements. However, there is still good correspondence with measured data, because it seems from Fig. 8 that the intercept of the x-axis at 7.1 mm is in the middle of the recorded rainfall events that produced no runoff. Finally, the linear model has a slope of 0.18, which corresponds to the runoff coefficient for the measurement area. Consequently, the linear model states that 18% of rainfall discharges if the soil volumetric water content exceeds $0.34 \text{ m}^3 \text{ H}_2\text{O m}^{-3}$ soil and if the accumulated rainfall exceeds an initial loss of 7.1 mm.

Discussion

Dunne and Black (1970a) and Kirkby and Chorley (1967) concluded that rainfall-runoff from permeable hill slopes is produced by wet spot (saturation excess) runoff and subsurface throughflow. Rainfall-runoff observed in this study show the same dynamics. Saturated areas near the line drain seem to produce short-term peaks during rainfall, while subsurface throughflow generates runoff in an extended time afterward. Subsurface throughflow seems to be the primary contributor to runoff and occurs when the soil water content is high. High soil water content is necessary to produce subsurface throughflow as this increases horizontal water transport in the soil. Measured soil water content at the bottom of a hill is highly correlated with produced runoff. This indicates that water is first transported across this point within the soil before reaching the soil surface and, thereby, the line drain. The soil characteristics of the area could further induce horizontal water transport in the soil

© ASCE

04019022-8

J. Hydrol. Eng.

since a siltier soil is present at a depth of 46 cm. Furthermore, the soil will supposedly be prone to higher compaction at a depth of 46 cm, which will reduce the effective porosity. Due to a higher silt content and soil compaction, the soil layer at a depth of 46 cm will have a lower infiltration capacity than the topsoil layer and, therefore, in some periods become a barrier to vertical water transport in the soil. This forces water to move horizontally.

During most of the year, there is a potential for surface runoff from the urban green area in Lystrup. According to Fig. 5, the soil water content is 0.34 $m^3 H_2O m^{-3}$ soil or above from September until July. This is a high soil water content that is relatively close to the average total porosity of 0.43, which locally is as low as 0.37. The high soil volumetric water content is probably maintained in this period due to low evapotranspiration during fall and winter. Comparatively, during late spring and summer, the soil water content is significantly reduced and reaches values as low as 0.13–0.20 $m^3 H_2O m^{-3}$ soil in the upper soil layer. In this way, a significant storage volume is available during spring and summer that will be exhausted only if the soil volumetric water content reaches 0.34 $m^3 H_2O m^{-3}$ soil again.

Several rainfall events are seen to produce runoff at the field station in Lystrup. None of these rainfall events exceeded the measured infiltration capacity of the topsoil, which in this case is the saturated hydraulic conductivity of 1.1 $mm min^{-1}$. This indicates that runoff is produced primarily because rainfall exceeds the water storage capacity of the topsoil as the infiltration capacity of the lower soil layer is exceeded. The water storage capacity, ΔS (mm), of the soil is dependent on the soil water content and can be written in the form of a simple mass balance in Eq. (6):

$$\Delta S = (\theta_{sc} - \theta)d_s \tag{6}$$

where θ_{sc} ($m^3 H_2O m^{-3}$ soil) = soil volumetric water content at maximum storage capacity before mobilization of horizontal water transport in soil; θ ($m^3 H_2O m^{-3}$ soil) = initial soil volumetric water content; and d_s (mm) = depth of soil body capable of storing water. If $\theta < \theta_{sc}$, there is an excess water storage capacity and horizontal water transport will not be significant. For example, under dry conditions, as seen in the summer where the soil volumetric water content reaches $\theta = 0.15$ $m^3 H_2O m^{-3}$ soil, there is an excess storage volume up to $\theta_{sc} = 0.34$ $m^3 H_2O m^{-3}$ soil, whereas the storage capacity according to the measurements is exhausted. The difference in soil water content is multiplied by the depth of the topsoil layer in Lystrup, which is $d_s = 460$ mm. This results in a temporary storage capacity at this point in time of 97 mm. The theory presented in Eq. (6) is confirmed by measurements where runoff is not produced below an average soil volumetric water content of 0.34 $m^3 H_2O m^{-3}$ soil.

The measurements from the field station indicate that subsurface throughflow is present, and therefore both horizontal water transport in terms of throughflow and vertical water transport in terms of infiltration to deeper aquifers are essential to describe rainfall-runoff in Lystrup. Therefore, a two-dimensional model could be the best solution to model the measured runoff processes. In this case, Horton's infiltration equation or other one-dimensional infiltration models are not sufficient. Furthermore, a measured cloudburst of a 10-year return period produced no runoff. The reason that no runoff was produced is that the rainfall intensity was not high enough to exceed the infiltration capacity, and as the initial soil water content prior to the rainfall event was 0.30 $m^3 H_2O m^{-3}$ soil, and so below the critical soil volumetric water content of 0.34 $m^3 H_2O m^{-3}$ soil, there were also storage capacity left in the soil to store rainfall in the soil matrix. In general, this rainfall event is an indication that rainfall intensities must be relatively

large to cause infiltration excess overland flow in Lystrup. Future experiments will investigate which rainfall characteristics are needed to generate infiltration excess overland flow in Lystrup.

To assess the runoff dynamics due to infiltration excess overland flow, it is necessary to use other means such as rainfall simulators if the natural rainfall intensity does not exceed the infiltration capacity. Rainfall simulators are generally designed to study high-intensity rainfall and how this affects infiltration excess runoff and processes related to this type of runoff. However, rainfall simulators would not be able to study subsurface throughflow because this requires the entire catchment to be hydrologically mobilized. This would simply require an unrealistic amount of water if such hydrological conditions should be reached with a rainfall simulator. Therefore, this study supplements rainfall simulator studies well because it can be used to study throughflow effects, while the rainfall simulators can be used to study infiltration excess overland flow. The disadvantage of this large-scale study is the missing ability to produce desired rainfall characteristics, which means that infiltration excess runoff will rarely be observed in this case.

The field station gives insights on where to locate soil sensor equipment in other research locations. Within the field station in Lystrup, the bottom hill sensor cluster showed the best correlation to the dynamics of generated runoff. Therefore, the most useful data are collected closest to the outlet of the catchment. This is expected because the bottom hill sensor cluster measures the result of all hydrological processes occurring within the hill slope. Although the uphill sensor clusters showed weaker correlations with the runoff, they are still important to indicate the average soil water content of the hill to estimate the total water storage capacity of the soil body.

The field station developed in this project collects and monitors all runoff reaching the line drain at the soil surface. The result of this can be that several types of runoff are mixed, for example, that subsurface throughflow is mixed with infiltration excess overland flow. In this way, it could be difficult to separate one runoff type from another and qualitatively quantify them. Future studies could put more emphasis on separating runoff types in the field by separating the surface from the subsurface. However, measuring the subsurface throughflow within the subsurface could lead to measuring throughflow that would have stayed in the subsurface and at a later point infiltrate to deeper aquifers.

Practical Applications

Accumulated runoff increases linearly as a function of accumulated rainfall if the soil volumetric water content is above 0.34 $m^3 H_2O m^{-3}$ soil and an initial loss of 7.1 mm is exceeded. Under these conditions, the runoff coefficient is 0.18. This can be utilized for further modeling of rainfall-runoff in Lystrup. Such a model will be helpful to

- estimate rainfall-runoff from urban green areas to stormwater detention ponds;
- estimate the baseflow produced by urban green area rainfall runoff in urban drainage networks as rainfall-runoff from urban green areas occur over several days; this could decrease the discharge capacity of the drainage networks during combined rainfall events; and
- estimate rainfall-runoff to wastewater treatment plants as these often have real-time-controlled cleaning processes depending on the relative concentration of sewage at the inlet to the plant.

In urban drainage engineering, one-dimensional infiltration models have the broadest application. In many cases, though, rainfall-runoff from green areas is neglected. It has been realized

that rainfall-runoff from the hill slope in Lystrup is more complicated than expected. This is because the runoff processes are controlled within the topsoil, as opposed to the runoff occurring directly at the soil surface. This result will help engineers to interpret and understand the hydrological processes in urban green areas and how this type of runoff should be included in the design of urban drainage systems and wastewater-treatment plants. This study has presented a robust method to monitor surface runoff directly from urban green surfaces, which will help future research projects to conduct similar experiments. However, the results in this study cannot generalize how green surfaces contribute to total runoff to urban drainage systems because of its limited geographical scale. Therefore, it is difficult to extrapolate the current data; more empirical attempts will be necessary to investigate the underlying runoff processes necessary for qualitative runoff estimation from urban green areas.

Conclusion

It has been found that an urban green area in Lystrup, Denmark, frequently contributes to runoff. The following characteristics of runoff were found:

- Runoff is only present at soil volumetric water contents above $0.34\ m^3H_2O/m^3$ soil.
- If rainfall occurs at a soil volumetric water content above $0.34\ m^3H_2O/m^3$ soil, an initial loss of 7.1 mm must be exceeded before runoff starts.
- The runoff coefficient of the area is 0.18 if the soil volumetric water content is above $0.34\ m^3H_2O/m^3$ soil and an initial loss of 7.1 mm is exceeded.
- Runoff most probably occurs as subsurface throughflow.

The results of this study agree with other large-scale studies carried out in rural areas. Generally, infiltration excess overland flow was not present, which is often assumed in the terms of Horton's infiltration theory. This indicates that engineers and scientists should be careful when deciding which runoff mechanism is the most dominant in urban green areas. Furthermore, as infiltration excess overland flow is often assumed to be dominant, it will be necessary in future studies to revisit current models used in design practice and determine whether the current assumptions and models for urban green area rainfall-runoff are reliable.

Future studies are necessary to develop both engineers' and scientists' knowledge of this field as urban green area rainfall-runoff can be crucial for optimal urban drainage design. Therefore, future research projects in urban environments are highly recommended. They can be conducted as large-scale experiments but also with small-scale rainfall simulator studies, which are often used to study runoff processes in rural and agricultural areas.

References

ACO Nordic. 2014. "ACO self liniedræn omkring huset—fleksibel. enkel. elegant." Accessed March 18, 2019. http://www.aco.dk/media/1681802 /ACO%20Self-Hex2,0%20brochure%202014.pdf.

Arriaga, F., T. Kornecki, K. Balkcom, and R. Raper. 2010. "A method for automating data collection from a double-ring infiltrometer under falling head conditions." *Soil Use Manage.* 26 (1): 61–67. https://doi.org /10.1111/j.1475-2743.2009.00249.x.

ASCE Task Committee on Application of Artificial Neural Networks in Hydrology. 2000. "Artificial neural networks in hydrology. II: Hydrologic applications." *J. Hydrol. Eng.* 5 (2): 124–137. https://doi .org/10.1061/(ASCE)1084-0699(2000)5:2(124).

Ashman, M., and G. Puri. 2013. *Essential soil science: A clear and concise introduction to soil science*. New York: Wiley.

Benavides Solorio, J., and L. H. MacDonald. 2001. "Post-fire runoff and erosion from simulated rainfall on small plots, Colorado front range." *Hydrol. Process.* 15 (15): 2931–2952. https://doi.org/10.1002/hyp.383.

Boyd, M. J., M. C. Bufill, and R. M. Knee. 1994. "Predicting pervious and impervious storm runoff from urban drainage basins." *Hydrol. Sci. J.* 39 (4): 321–332. https://doi.org/10.1080/02626669409492753.

Boyd, M. J., M. C. Bufill, and R. M. Knee. 2009. "Pervious and impervious runoff in urban catchments." *Hydrol. Sci. J.* 38 (6): 463–478. https://doi .org/10.1080/02626669309492699.

Brocca, L., F. Melone, T. Moramarco, and V. P. Singh. 2009. "Assimilation of observed soil moisture data in storm rainfall-runoff modeling." *J. Hydrol. Eng.* 14 (2): 153–165. https://doi.org/10.1061/(ASCE)1084 -0699(2009)14:2(153).

Campbell Scientific. 2010. "ARG100 tipping bucket rain gauge." Accessed March 18, 2019. https://s.campbellsci.com/documents/eu/manuals /arg100.pdf.

Campbell Scientific. 2014. "CS451/CS456 submersible pressure transducer." Accessed March 18, 2019. https://s.campbellsci.com/documents /us/manuals/cs451-cs456.pdf.

Cerdà, A., S. Ibáñez, and A. Calvo. 1997. "Design and operation of a small and portable rainfall simulator for rugged terrain." *Soil Technol.* 11 (2): 163–170. https://doi.org/10.1016/S0933-3630(96)00135-3.

Clarke, M. A., and R. P. D. Walsh. 2007. "A portable rainfall simulator for field assessment of splash and slopewash in remote locations." *Earth Surf. Process. Landforms* 32 (13): 2052–2069. https://doi.org/10 .1002/esp.1526.

Dane, J. H., and G. C. Topp. 2002. *Methods of soil analysis, Part 4— Physical methods*. Madison, WI: Soil Science Society of America.

Decagon Devices. 2015. "MPS-2 & MPS-6—Dielectric water potential sensors." Accessed March 18, 2019. http://www.edaphic.com.au/wp -content/uploads/2018/01/MPS-6-Manual.pdf.

Decagon Devices. 2016. "5TE—Water content, EC and temperature sensor." Accessed March 18, 2019. http://manuals.decagon.com /Retired%20and%20Discontinued/Manuals/13509_5TE_Web.pdf.

Dunne, T., and R. D. Black. 1970a. "An experimental investigation of runoff production in permeable soils." *Water Resour. Res.* 6 (2): 478–490. https://doi.org/10.1029/WR006i002p00478.

Dunne, T., and R. D. Black. 1970b. "Partial area contributions to storm runoff in a small new england watershed." *Water Resour. Res.* 6 (5): 1296–1311. https://doi.org/10.1029/WR006i005p01296.

ecoTech Umwelt-Meßsysteme. 2014. "TensioMark—Manual for installation and use of TensioMarks." Accessed March 18, 2019. https:// www.stevenswater.com/resources/documentation/Stevens_Tensiomark _Manual.pdf.

Govindaraju, R. S. 2000. "Artificial neural networks in hydrology. I: Preliminary concepts." *J. Hydrol. Eng.* 5 (2): 115–123. https://doi .org/10.1061/(ASCE)1084-0699(2000)5:2(115).

Grayson, R. B. 1997. "Preferred states in spatial soil moisture patterns: Local and nonlocal controls." *Water Resour. Res.* 33 (12): 2897–2908. https://doi.org/10.1029/97WR02174.

Green, W. H., and G. A. Ampt. 1911. "Studies on soil physics." *J. Agric. Sci.* 4 (1): 1–24. https://doi.org/10.1017/S0021859600001441.

Gregory, J. H. 2006. "Effect of urban soil compaction on infiltration rate." *J. Soil Water Conserv.* 61 (3): 117–124.

Groenendyk, D. G., T. P. A. Ferré, K. R. Thorp, and A. K. Rice. 2015. "Hydrologic-process-based soil texture classifications for improved visualization of landscape function." *PLoS One* 10 (6): e0131299. https://doi.org/10.1371/journal.pone.0131299.

Horton, R. E. 1939. "Analysis of runoff-plat experiments with varying infiltration-capacity." *Eos Trans. Am. Geophys. Union* 20 (4): 693–711. https://doi.org/10.1029/TR020i004p00693.

Humphry, J. B. 2002. "A portable rainfall simulator for plot-scale runoff studies." *Appl. Eng. Agric.* 18 (2): 199–204. https://doi.org/10.13031/2013.7789.

Jacobs, J. M., D. A. Myers, and B. M. Whitfield. 2003. "Improved rainfall/runoff estimates using remotely sensed soil moisture." *J. Am. Water Resour. Assoc.* 39 (2): 313–324. https://doi.org/10.1111/j.1752-1688.2003.tb04386.x.

Kale, R. V., and B. Sahoo. 2011. "Green-AMPT infiltration models for varied field conditions: A revisit." *Water Resour. Manage.* 25 (14): 3505–3536. https://doi.org/10.1007/s11269-011-9868-0.

Kirkby, M. J., and R. J. Chorley. 1967. "Throughflow, overland flow and erosion." *Bull. Int. Assoc. Sci. Hydrol.* 12 (3): 5–21. https://doi.org/10.1080/02626666709493533.

Madsen, H., I. B. Gregersen, D. Rosbjerg, and K. Arnbjerg-Nielsen. 2017. "Regional frequency analysis of short duration rainfall extremes using gridded daily rainfall data as co-variate." *Water Sci. Technol.* 75 (8): 1971–1981. https://doi.org/10.2166/wst.2017.089.

Pan, C., and Z. Shangguan. 2006. "Runoff hydraulic characteristics and sediment generation in sloped grassplots under simulated rainfall conditions." *J. Hydrol.* 331 (1–2): 178–185. https://doi.org/10.1016/j.jhydrol.2006.05.011.

Pilgrim, D. H., D. D. Huff, and T. D. Steele. 1978. "A field evaluation of subsurface and surface runoff." *J. Hydrol.* 38 (3–4): 319–341. https://doi.org/10.1016/0022-1694(78)90077-X.

Poulsen, T. G., P. Moldrup, T. Yamaguchi, and O. H. Jacobsen. 1999. "Predicting saturated and unsaturated hydraulic conductivity in undisturbed soils from soil water characteristics." *Soil Sci.* 164 (12): 877–887. https://doi.org/10.1097/00010694-199912000-00001.

Quinton, J. N., G. Edwards, and R. Morgan. 1997. "The influence of vegetation species and plant properties on runoff and soil erosion: Results from a rainfall simulation study in south east Spain." *Soil Use Manage.* 13 (3): 143–148. https://doi.org/10.1111/j.1475-2743.1997.tb00575.x.

Redfern, T. W., N. MacDonald, T. R. Kjeldsen, J. D. Miller, and N. Reynard. 2016. "Current understanding of hydrological processes on common urban surfaces." *Prog. Phys. Geogr.* 40 (5): 699–713. https://doi.org/10.1177/0309133316652819.

Ribolzi, O., J. Patin, L. M. Bresson, K. O. Latsachack, E. Mouche, O. Sengtaheuanghoung, N. Silvera, J. P. Thiébaux, and C. Valentin. 2011. "Impact of slope gradient on soil surface features and infiltration on steep slopes in northern Laos." *Geomorphology* 127 (1–2): 53–63. https://doi.org/10.1016/j.geomorph.2010.12.004.

Sentek. 2015. "Sentek drill & Drop SDI-12 series 3." Accessed March 18, 2019. http://www.sentek.com.au/downloads/downloads.asp?TypeID=13&FolderID=22.

Sharma, K. D. 1986. "Runoff behaviour of water harvesting microcatchments." *Agric. Water Manage.* 11 (2): 137–144. https://doi.org/10.1016/0378-3774(86)90026-0.

Sharpley, A. 2003. "Effect of rainfall simulator and plot scale on overland flow and phosphorus transport." *J. Environ. Qual.* 32 (6): 2172–2179. https://doi.org/10.2134/jeq2003.2172.

Shuster, W. D., E. Pappas, and Y. Zhang. 2008. "Laboratory-scale simulation of runoff response from pervious-impervious systems." *J. Hydrol. Eng.* 13 (9): 886–893. https://doi.org/10.1061/(ASCE)1084-0699(2008)13:9(886).

Thorndahl, S., K. J. Beven, J. B. Jensen, and K. Schaarup-Jensen. 2008. "Event based uncertainty assessment in urban drainage modelling, applying the GLUE methodology." *J. Hydrol.* 357 (3–4): 421–437. https://doi.org/10.1016/j.jhydrol.2008.05.027.

Thorndahl, S., C. Johansen, and K. Schaarup-Jensen. 2006. "Assessment of runoff contributing catchment areas in rainfall runoff modelling." *Water Sci. Technol.* 54 (6–7): 49–56. https://doi.org/10.2166/wst.2006.621.

YDOC (Your Data Our Care). 2016. "YDOC data logger manual." Accessed March 18, 2019. http://www.your-data-our-care.com/download/YDOC-Datalogger%20Manual.pdf.